JOURNAL OF SOLID STATE CHEMISTRY 75, 60–72 (1988)

The Solvolytic Disproportionation of Mixed-Valence Compounds

II. $Tb_{11}O_{20}$

Z. C. KANG AND L. EYRING

Department of Chemistry and the Center for Solid State Science, Arizona State University, Tempe, Arizona 85287

Received June 15, 1987; in revised form January 4, 1988

The intermediate higher oxides of terbium are solvolytically disproportionated in acid solution to yield Tb^{3+} (aq) ions and a residue of TbO_2(c). The starting material and the final solid product have fluorite-like structures requiring no reconstruction of the cation substructure. $Tb_{11}O_{20}$ was leached with a mixture of concentrated hydrochloric and acetic acids and the product examined utilizing electron microscopy to reveal the mechanism of the reaction. It is apparent that all the oxide is dissolved from selected reaction pits to yield Tb^{3+} (aq) ions and H_2O. This dissolution is accompanied by oxygen transport into remote regions where $Tb_{11}O_{20}$ is oxidized to TbO_2. This forms an insoluble skeletal fragment of the original crystal. The reaction pits occur at dislocation/surface intersections.

Introduction

In the previous paper the mechanism of solvolytic disproportionation of Pr_7O_{12} in dilute acid was discussed (*1*). It was found that coupled reactions accounted for the leaching process. As the solution of the trivalent ions occurred the reduction of the contiguous tetravalent ions, accompanied by the transport of oxygen, resulted in the removal of all the oxide from the reacting region. This process enables the concomitant oxidation of part of the remaining crystal to PrO_2 at some distance away. In this paper we compare this behavior with that of the analogous terbium oxide system.

Solvolytic disproportionation of TbO_x has been reported previously (*2–4*). In these studies it was found that the process was so slow under the conditions effective for PrO_x that a more reactive environment had to be provided. The net result at the macroscopic level, however, was similar. Pure TbO_2 with a lattice parameter a = 5.220 Å was obtained. In fact, this is the only method that provides pure TbO_2 in substantial amounts (*4*).

The reaction to be reported here involves a composition of approximately $TbO_{1.75}$ which is a mixture of Tb_7O_{12} and $Tb_{11}O_{20}$. The structures of these two compounds are fluorite related and the solid reaction product is TbO_2 (which has the fluorite structure). The proposed structure of $Tb_{11}O_{20}$ is illustrated in Fig. 1. The tri- and tetravalent ions of Tb are present in the same basic cluster as in $PrO_{2-\delta}$ (*1*). There is no heterogeneity at a higher level, thus the reaction requires a reduction at the reaction site with an oxidation at some distant location.

Experimental Part

The terbium oxide was purchased from Research Chemicals Inc. as 99.999% pure as an oxalate ignition product. This material was placed in a muffle furnace at 1000°C

0022-4596/88 $3.00

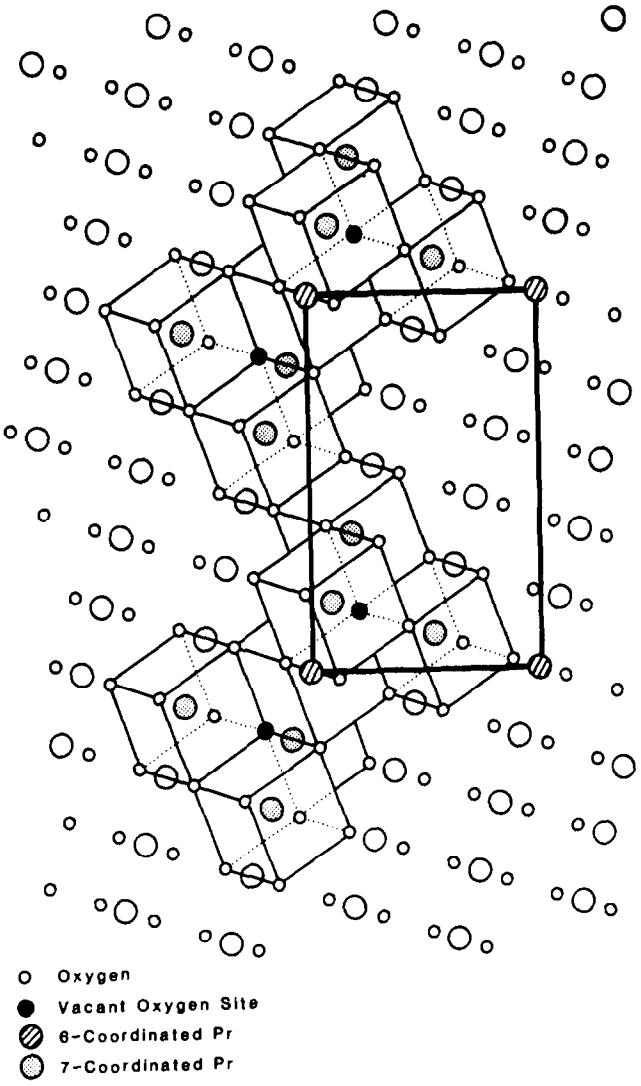

FIG. 1. A projection of the proposed unit cell of $Tb_{11}O_{20}$ along ⟨211⟩ (heavy solid lines). All the terbium atoms are cubically coordinated with oxygen in the fluorite structure as suggested by the cubes drawn about some of them. In $Tb_{11}O_{20}$ there are two vacant oxygen sites in each unit cell. The metal atoms chosen to be the corners of the unit cell are six-coordinated while all the others are either seven- or eight-coordinated.

for 12 hr then allowed to cool slowly to 200°C before removing it to a desiccator for further treatment. The two-phase mixture of Tb_7O_{12} and $Tb_{11}O_{20}$ thus obtained yielded the broad-lined powder diffraction pattern shown in Fig. 2.

The mixture was treated with equal parts by volume of concentrated hydrochloric acid and glacial acetic acid at boiling temperatures for 5 to 40 min. The product was red-brown in color and shown to be TbO_2 by X-ray diffraction analysis (Fig. 2). Some

samples were treated for shorter times so that the reaction could be arrested in progress.

Specimens to be observed in the microscope were dispersed in dry acetone and a drop of the suspension applied to a holey carbon film supported on a microscope grid for drying. The specimens thus prepared were examined in a JEM 200CX high-resolution microscope fitted with a top-entry stage and with a double-tilt specimen holder. The electron source is LaB_6. It is equipped with a TV image pick-up and viewing system.

Results

The diffraction patterns of the final product were indexed as fluorite with $a_{TbO_2} = 5.215 + 0.002$ Å (compared to $a_{TbO_2} = 5.220 \pm 0.003$ Å by Brauer and Pfeiffer (*2*). The pattern, as shown in Fig. 2, is sharp with no extra lines. This does not preclude the possibility of very small amounts of undetected

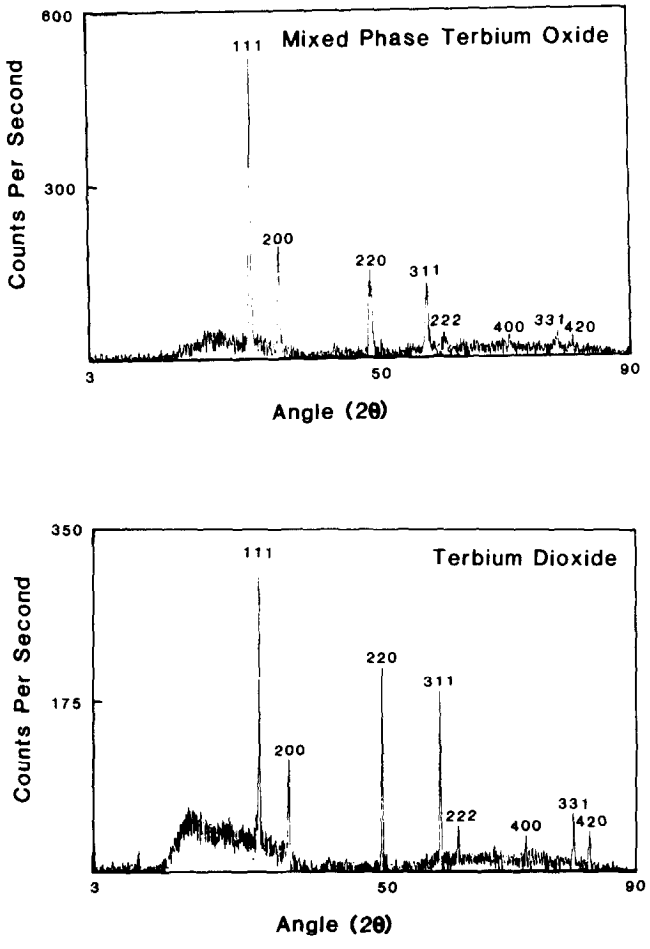

FIG. 2. A powder X-ray diffraction pattern of TbO_x (top). The broadened lines result from the two-phased mixture of Tb_7O_{12} and $Tb_{11}O_{20}$. A powder X-ray diffraction pattern of the product TbO_2 is at the bottom.

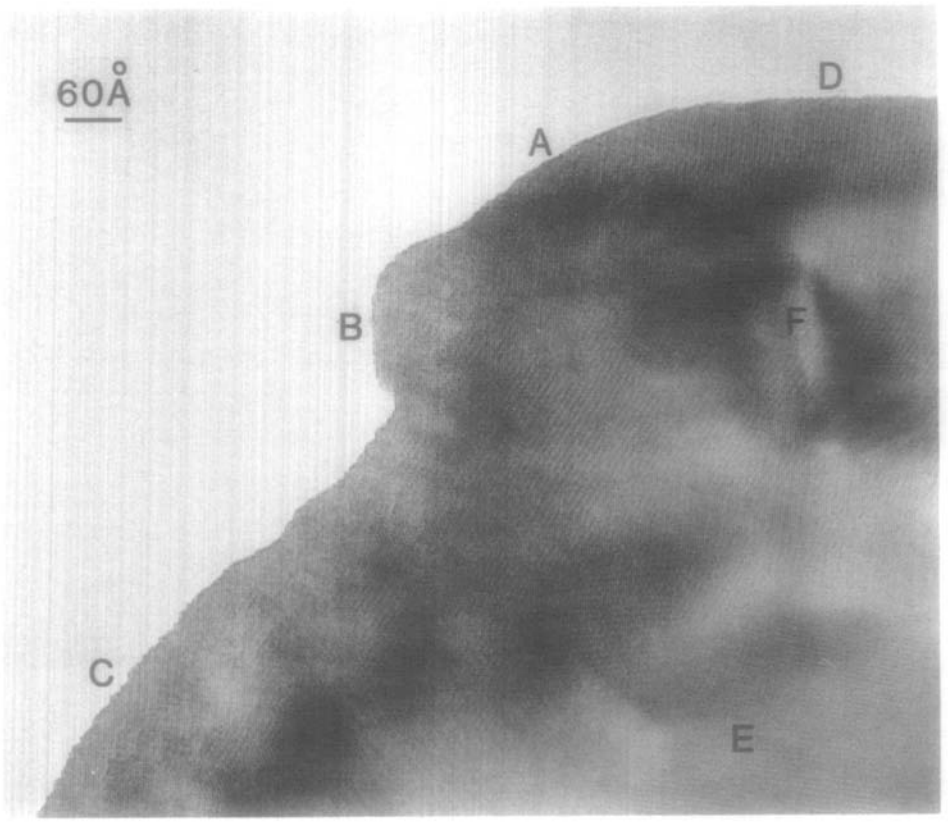

FIG. 3. A high-resolution image of the TbO_x starting material. The various surfaces and their morphology are labeled A, B, C, and D. Two dislocations are marked E and F.

lower oxides or hydrated products. There was no grinding or other alteration of the reactant or product microcrystals before observation in the electron microscope. A high-resolution image of one of the crystals of the TbO_x starting material is shown in profile in Fig. 3. Several characteristics should be commented upon. This is a $[110]_F$ (F refers to fluorite) zone image so that the rows of spots in the array correspond to columns of terbium atoms deployed along $(111)_F$ planes.

Extended regions of straight surface occur with the (111) planes at points A and B. The rest of the surface profile consists of either a rather irregular line of (111) steps in the curve at C or a nearly straight portion at D that is approximately $(13\bar{3})$ with some small irregularity. These observations have already been discussed in detail elsewhere (*5*).

The other major feature to be noticed is the low concentration of dislocations, for example, at F. These dislocations, which have been characterized (*6*) as $1/6\ [2\bar{1}\bar{1}]\ (1\bar{1}1)$, are no doubt the site of the observed leaching reaction to be described. It is very likely that these dislocations carry a charge due to the interruption of the regularly placed ionic charges in the perfect crystal.

Images of typical TbO_2 product crystals after the leaching of TbO_x by the acid solution are shown in Figs. 4a and 4b. The leach pit, in Fig. 4a, is clearly outlined by Fresnel

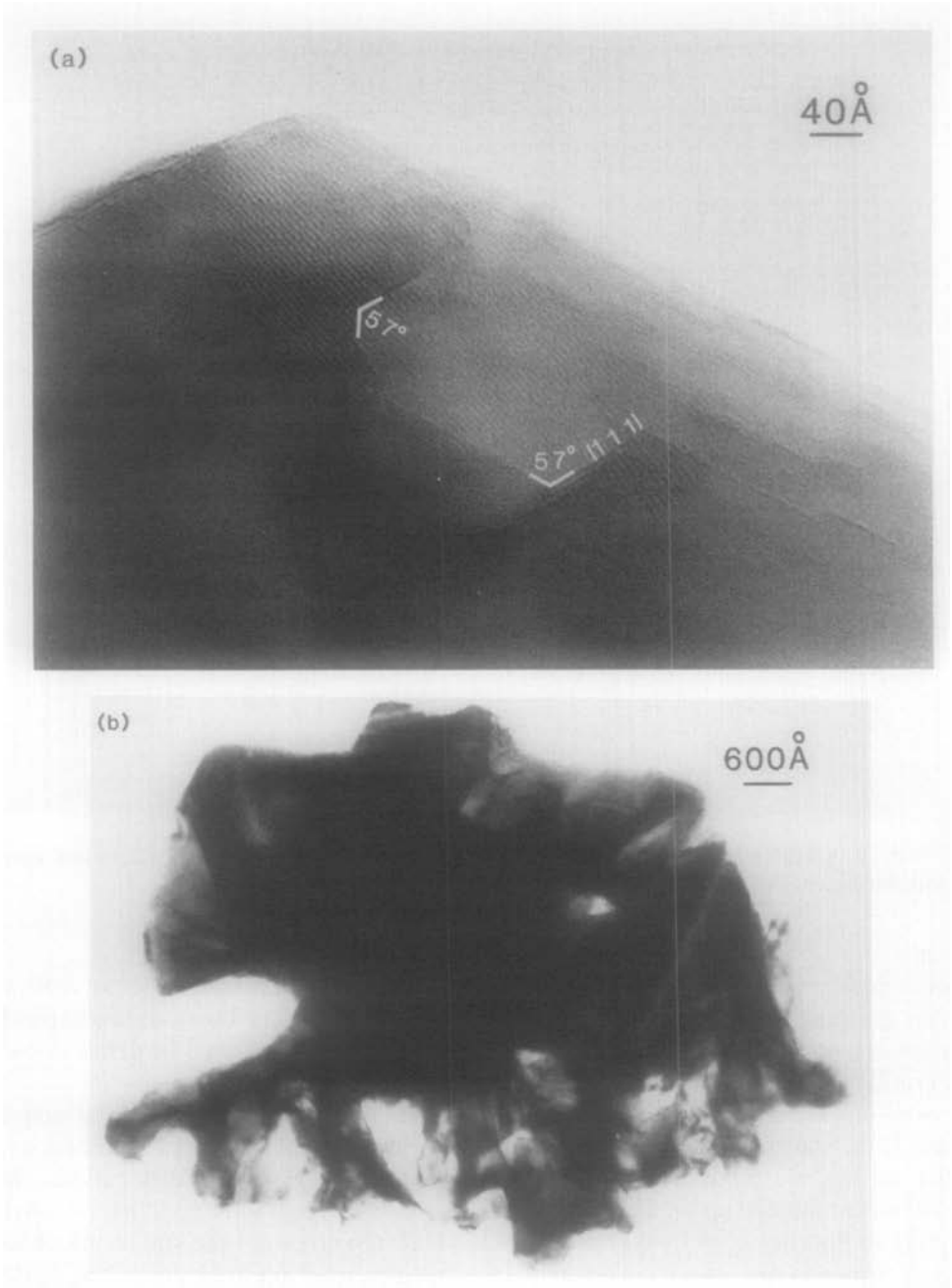

FIG. 4. The morphology of chemically leached TbO_x. (a) A leach pit developed with (111) walls in the early stages of reaction. (b) The final product consisting of a network of TbO_2 material enclosing fully developed leach pits.

fringes as are the major surface steps of the crystal. The crystal is just off a ⟨110⟩ zone and the contours of the leach pit and the edges are generally {111} planes. The angle between the facets is 57°, characteristic of the intersection of {111} planes in the fluo-

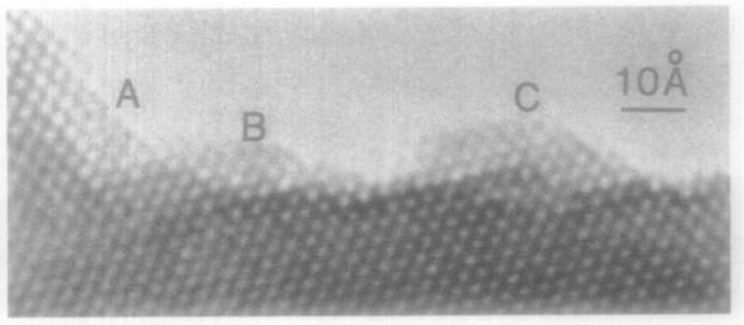

FIG. 5. A white-dot surface profile image from a leached sample. Notice the predominant (111) edge at A. Relics of the reaction remain at B and C.

rite structure. The studies of dynamic effects in thin edges in TbO_x (7) indicated that the {111} edges were the least active in the electron beam in vacuum. It is apparent that they behave in a similar benign way in the solution attack and that reaction on, for example, {110} or {211} planes is more vigorous. Figure 4b shows the final product of leaching of a TbO_x crystal after boiling it in a solution of equal parts concentrated HCl and glacial HAc. This low-magnification image shows the selective multidimensional nature of the attack.

The edge of a leached TbO_2 crystal is shown with high resolution in Fig. 5. There is a reasonably straight {111} planar edge on the left. The role of the {111} planes are emphasized in the development of the rest of the surface. The varied contrast in the atomic rows appearing as white dots at the surface is due to the different numbers of atoms in the surface rows. It is clear that the centers of some atomic rows are displaced from surface positions extrapolated from the bulk.

It is to be expected that the remnants of the leaching reaction should be evident in the thin surface profiles of the TbO_2 product. This is indeed the case. There are two types of residual features to be remarked upon. The first is that only the residues of dislocations are evident. (The dislocation density in the whole crystal has been reduced markedly.) For example, in Fig. 6 at A is the last vestige of an edge dislocation in which a reduced number of planes are in the surface. (The white dots are rows of Tb atoms.) The second type of residue of the

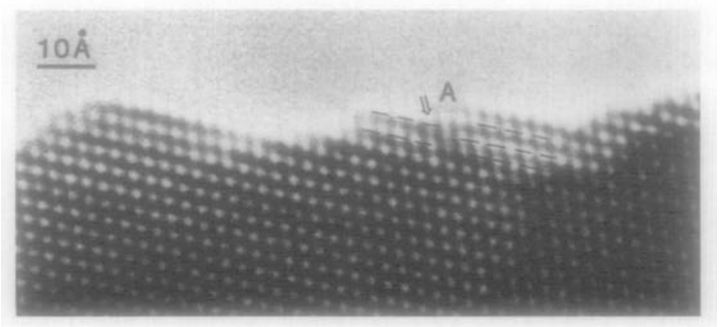

FIG. 6. A white-dot surface profile image of the edge of a leached crystal showing a remnant of a dislocation at A.

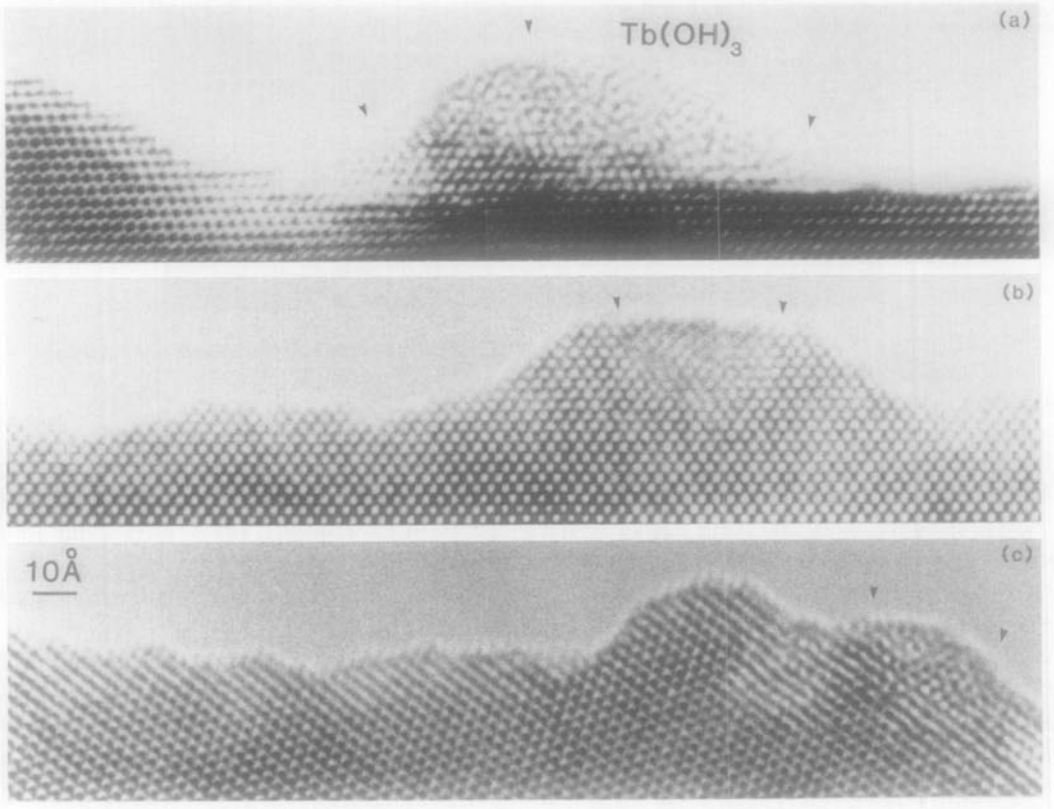

FIG. 7. Images of incompletely reacted surfaces. Notice in each of (a), (b), and (c) a raised portion that is highly disordered. The raised region is probably solvated and was in the process of dissolution.

reaction is illustrated in three examples in Fig. 7. In each example there are broadly raised regions believed to show a definite step in the dissolution process. It is clear that these raised parts of the crystal are generally disordered and almost amorphous in some regions. This suggests that projections that remain in an advancing reaction front first disorder, then dissolve, having freed oxygen to further oxidize the interior. The disordering would probably be due to the solvation of the transforming region.

The leaching reaction was arrested in some instances by removing crystals before the completion of the reaction and washing them in distilled water followed by an alcohol rinse. In these samples the pits frequently were not completely through the crystal yielding images of ordered intermediate phases. Sometimes the reaction went completely through the sample yielding thin-edged holes that could be studied at high resolution.

Figure 8a shows a diffraction pattern and in Fig. 8b an image of a thinning edge completely transformed to Tb_2O_3 (C-type) which would certainly have been leached away had the reaction been allowed to continue. The C-type sesquioxide is the end product of the reduction reaction, thus showing definitely that the excess oxygen originally present in this region has diffused away leaving a highly ordered region of Tb_2O_3.

Figure 9 shows the partially oxidized phases that are formed during dispropor-

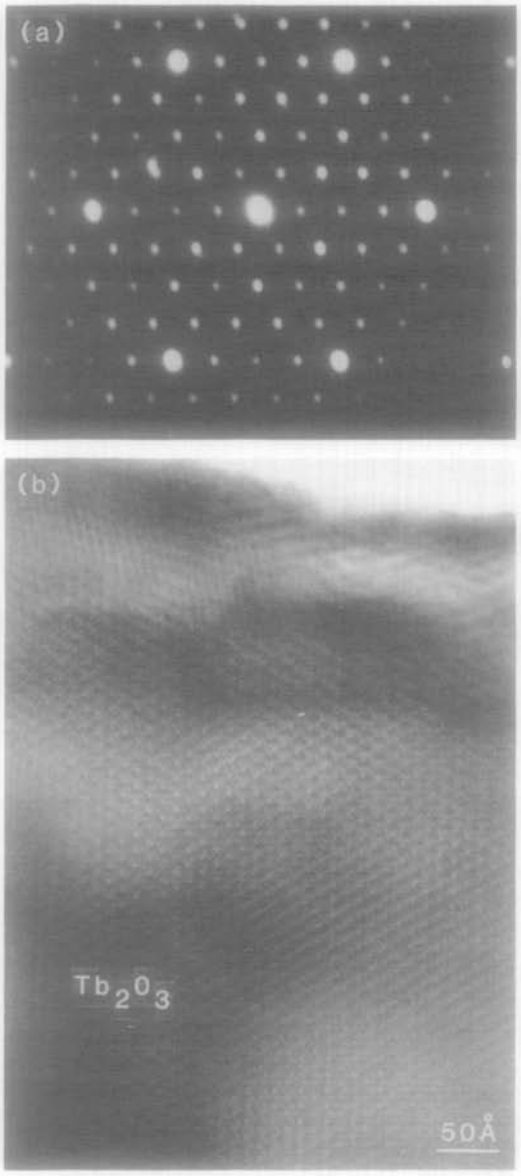

FIG. 8. A diffraction pattern (a) and the image (b) showing that, in the process of solvolytic disproportionation, regions of C-type Tb_2O_3 are formed prior to their dissolution.

tionation as the reaction proceeds to produce TbO_2. In Fig. 9a the thin regions marked A, B, and C show projected unit cells with 3, 4, and 8 atomic columns. These are orientational variants of the $\beta(2)$ form of $Tb_{24}O_{44}$. Figure 9b shows domains of the well-known $\beta(2)$ form of $Tb_{24}O_{44}$ in the thinned region at D. Region E is an orientational variant of region D and is an inverted image of region A of Fig. 9a having a projection of three atomic rows per unit cell.

To demonstrate that the regions marked A, B, C, and D of Figs. 9a and 9b are indeed orientational variants of $\beta(2)$, $Tb_{24}O_{44}$, optical diffraction patterns were obtained from each region of the micrographs. These patterns together with those calculated are shown in Fig. 10.

In some cases the reaction ended when the pit was virtually the full depth of the crystal as shown in Fig. 11. It appears that here two leach pits are developed on opposite sides of the crystal and only a thin layer of essentially TbO_2 remains; so thin in fact that a hole has appeared leaving very thin edges on its periphery. The edges of the pit are again primarily {111} planes. Fringes indicate compositional variation over the thin region.

An enlargement of the region of the hole appearing in Fig. 11 is shown in Fig. 12. The image is that of a TbO_2 crystal in the ⟨110⟩ zone. There are, however, some moiré fringes and other evidence of compositional variation even in this thin region. In only one small region of this profile image is there a reasonably straight edge and that is essentially along a {111} plane. However, most of the edges are formed roughly by {111} planes. The apparently amorphous regions on the surface and some areas with unmatched fringes may represent a residual unoxidized and probably solvated material as discussed above. Some surface steps also appear suggesting that the reaction occurs layer by layer one metal atom layer wide.

Discussion

The general outline of the leaching reaction in TbO_x is clearly parallel to that in PrO_x but with striking differences. The gen-

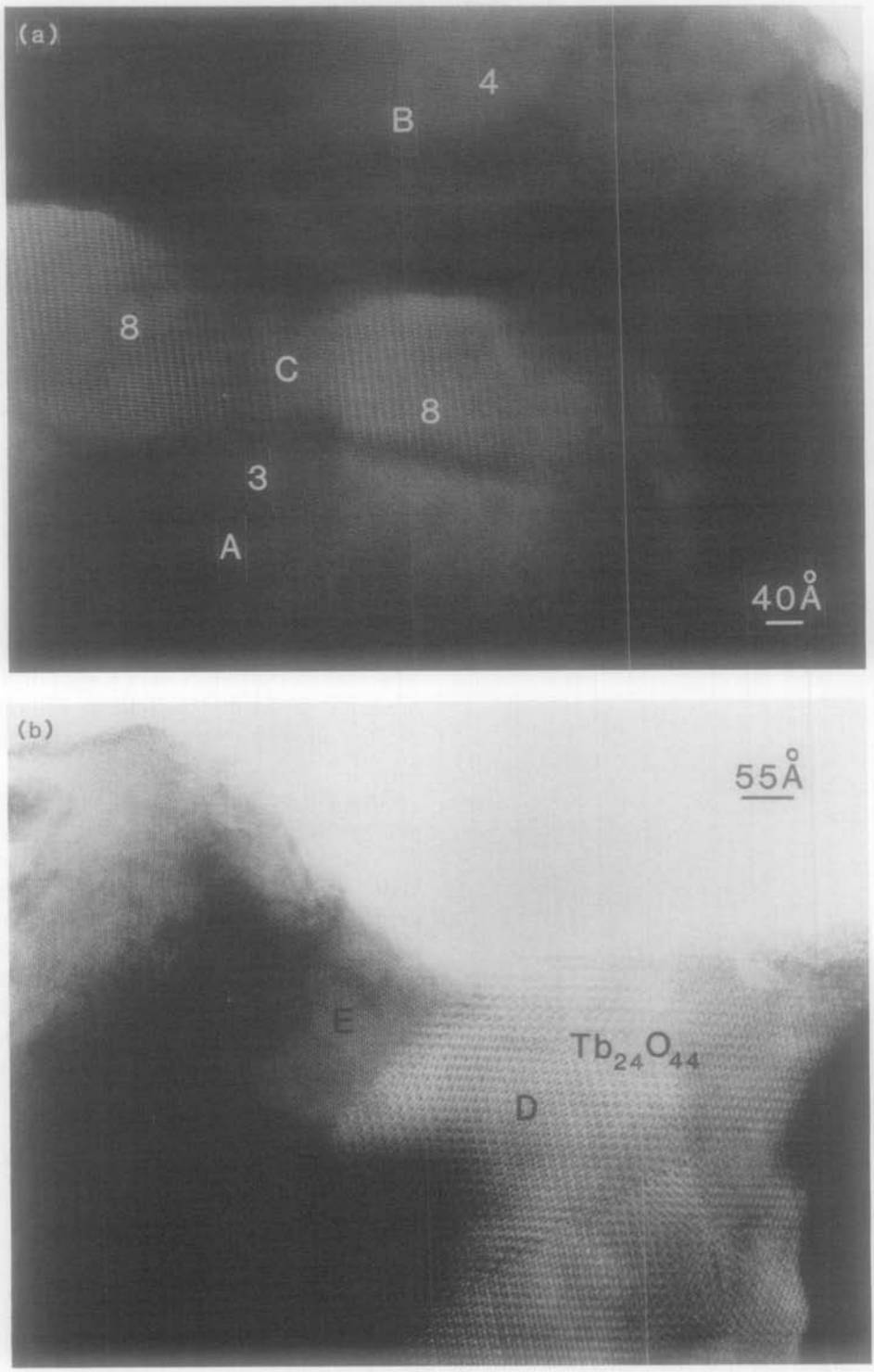

FIG. 9. High-resolution images of an oxidized intermediate phase formed during solvolytic disproportionation. (a) Three regions are marked A, B, and C where three orientational variants of $Tb_{24}O_{44}$ exist having 3-, 4- and 8-metal atom columns in the projected unit cell, respectively. (b) An image of domains of $Tb_{24}O_{44}$ in the [2$\bar{1}$1] zone, D, and the orientational variant, E, that is an inversion of that marked A in (a).

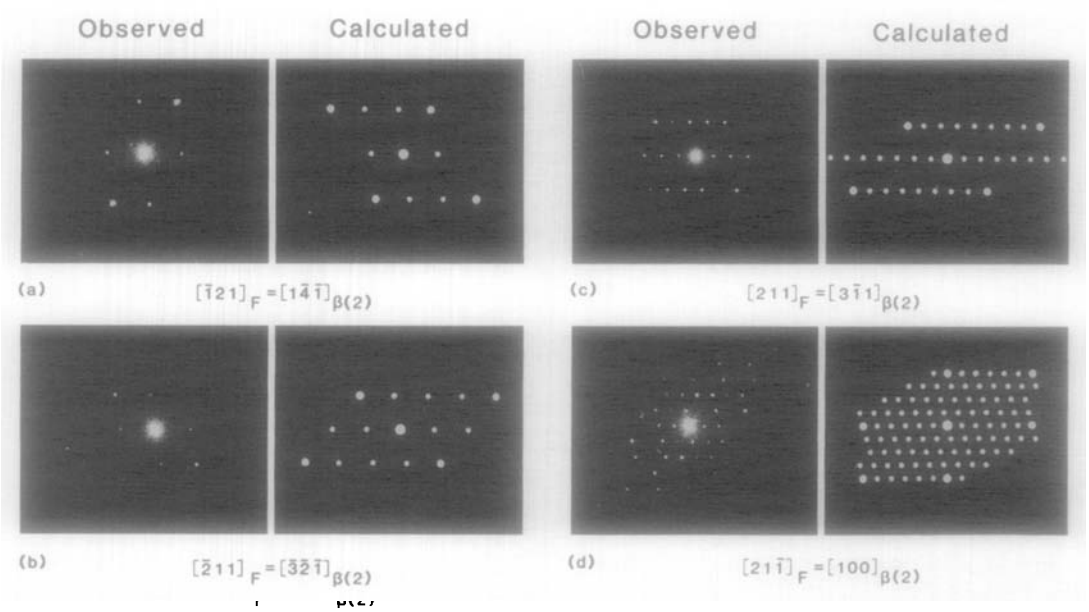

FIG. 10. Observed optical diffraction patterns and those calculated for the orientational variants of $\beta(2)$, $Tb_{24}O_{44}$. The parts (a), (b), (c), and (d) refer to the regions A, B, C, and D of Figs. 9a and 9b. The corresponding orientations between fluorite and $\beta(2)$ are indicated.

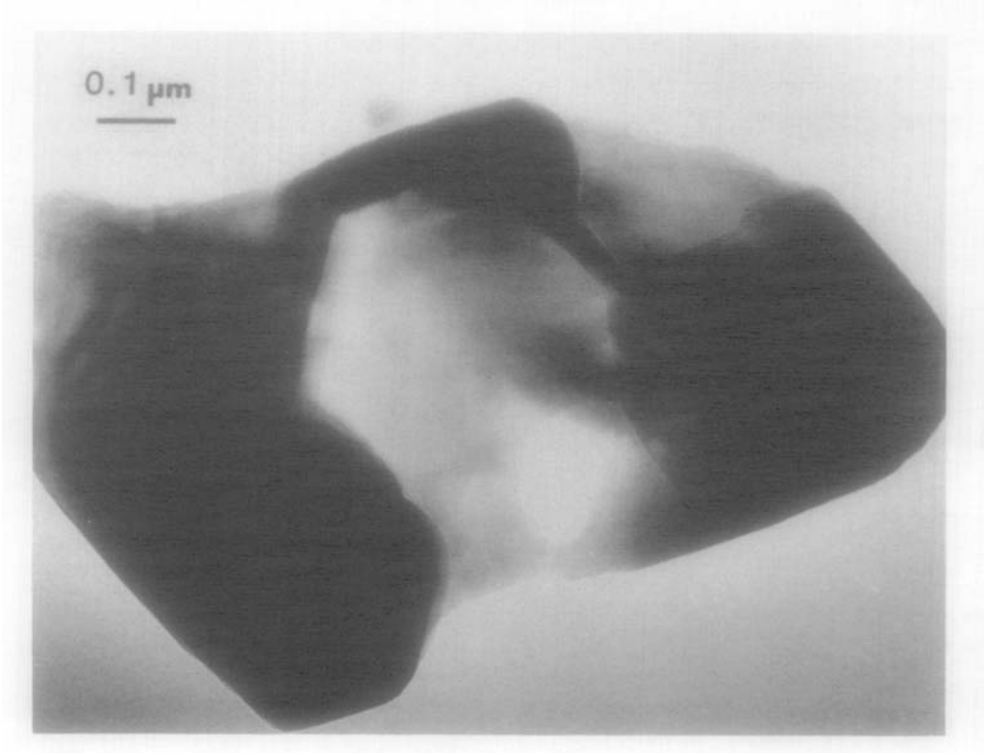

FIG. 11. A high-magnification image of a reacted fragment showing a fully developed leach pit with (111) walls.

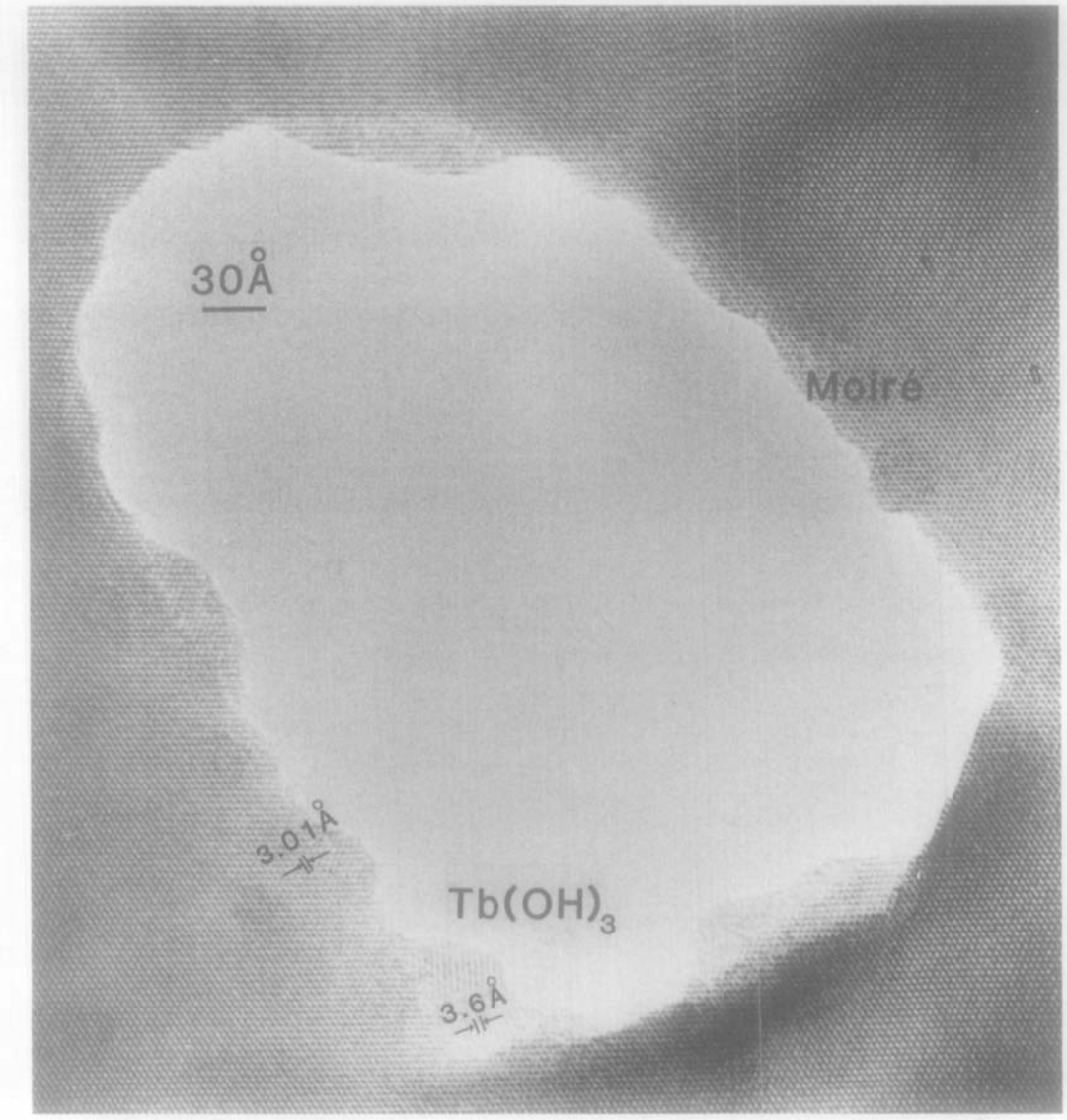

FIG. 12. A high-resolution image of the region of the leached hole of Fig. 10. Notice the moiré pattern at the right, the disordered projection at the bottom, and the region marked $Tb(OH)_3$ with considerable order, each suggesting incomplete oxidation.

eral reaction sequence must be the same; that is,

$$4/11Tb_{11}O_{20}(c) + 12H^+(aq) = 4Tb^{3+}(aq) + 6H_2O(l) + 14/11O(c), \quad (1)$$

followed by

$$7/11Tb_{11}O_{20}(c) + 14/11O(c) = 7TbO_2(c), \quad (2)$$

resulting in

$$Tb_{11}O_{20}(c) + 12H^+(aq) = 4Tb^{3+}(aq) + 7TbO_2(c) + 6H_2O(l). \quad (3)$$

Similar reactions can be represented if the oxygen species being transported is 0^- or $0^=$ with the concomitant transport of electrons in the opposite direction (*1*). One cannot settle the question of the species of oxygen transported in these experiments, thus none of the possibilities can be ruled out.

This reaction then allows the $Tb_{11}O_{20}$ to be completely removed from the reaction site and the valence disproportionation with oxygen transport that amounts to the reduction of Tb^{4+} at the surface and the corresponding oxidation of a Tb^{3+} ion in the interior. Thus, a pit forms at the easy reaction location.

The morphology of the final product shows a TbO_2 crystal with very broad pits having generally (111) walls (Fig. 11). This means that the (111) faces are less reactive during the solution reaction at the solid–liquid boundary as they are less kinetically active in a vacuum (*7*). The pits are postulated to arise from a reaction beginning at and following along a dislocation in the original crystal. These dislocations are clearly seen in Fig. 3, for example, at F and E. The pit in Fig. 4 has formed and has become broadened early in the reaction. This behavior is in marked contrast to that observed in PrO_x (*1*) where the pits are relatively long and narrow.

The conditions that produced leaching in PrO_x were ineffective in TbO_x. This behavior is consistent with the very much slower reaction of TbO_x with oxygen than the corresponding reaction with PrO_x commonly observed (*8*). Higher temperatures and quite different conditions are required for the solvolytic reaction for TbO_x (*2, 3*). The morphology of the solid-state reaction is observed to be distinctly different as well. In both cases, the intermediate oxides are removed from a localized reaction zone with an accompanying oxidation of the intermediate oxide at some nonleaching site. This requires the transport of oxygen along faults such as dislocations as well as through the bulk. The morphology of the leached pit reflects the balance of oxygen diffusion by these two routes. (Oxygen diffusion in Pr_7O_{12} is rapid (*9*) but no quantitative comparisons with TbO_x have been made.) It is clear that under conditions that produce leaching the ratio of oxygen transport in the bulk to that along defects is greater in TbO_x than in PrO_x since the pits in the PrO_2 product are deep and narrow while they are relatively broader in the TbO_2 product.

Another difference is in the conditions of the solvolytic attack. The leaching of PrO_x was carried out at room temperature whereas that of TbO_x was at about 100°C to achieve tractable reaction times. Of course, this reflects the larger reactivity of the more basic PrO_x to water and acids. The contrast in morphology of attack reflects these differences in the physical and chemical characteristics of PrO_x and TbO_x.

Conclusion

The solvolytic disproportionation attack by acidic water solution on $Tb_{11}O_{20}$ removes material from a reaction site (probably a surface-dislocation intersection). The removed material has the composition (and sometimes the structure) of Tb_2O_3. This requires that oxygen be transported from the reaction zone and effect a concomitant oxidation in a remote region of the crystal. The reaction as it progresses forms broad pits that reflect the relative resistance of the crystal faces to attack (i.e., the (111) faces are the less reactive). It will be important to examine other examples of solvolytic disproportionation where the crystal structures of reactant and product are incompatible and require a reconstructive solid-state transformation in the formation of the oxidized residue.

Acknowledgment

Financial support from the NSF through Research Grant DMR-8516381 and Grant DMR-8306501 which supports the high-resolution facility is gratefully acknowledged.

References

1. Z. C. KANG AND L. EYRING, *J. Solid State Chem.* **75,** 52 (1988).
2. G. BRAUER AND B. PFEIFFER, *Angew. Chem.* **1,** 551 (1962).
3. G. BRAUER AND B. PFEIFFER, *J. Less-Comm. Metals* **5,** 171 (1963).
4. A. F. CLIFFORD, *in* "Rare Earth Research II" (K. S. Vorres, Ed.), pp. 45–50, Gordon & Breach, New York (1964).
5. Z. C. KANG, D. J. SMITH, AND L. EYRING, *Surf. Sci.* **175,** 684 (1986).
6. Z. C. KANG AND L. EYRING, "Dislocations in Anion-Deficient Fluorite-Related Structures in Terbium Oxides," to be published.
7. Z. C. KANG, L. EYRING, AND D. J. SMITH, *Ultramicroscopy* **22,** 71 (1987).
8. E. D. GUTH AND L. EYRING, *J. Amer. Chem. Soc.* **76,** 5242 (1954).
9. K. H. LAU, D. L. FOX, S. H. LIN, AND L. EYRING, *High Temp. Sci.* **8,** 129 (1976).